The Raman fingerprint of plutonium dioxide: Some example applications for the detection of PuO2 in host matrices

Manara, D; Naji, M.; Mastromarino, S.; Elorrieta, J. M.; Magnani, Nicola; Martel, L.; Colle, J-Y

DOI
10.1016/j.jnucmat.2017.11.042

Publication date
2018

Document Version
Final published version

Published in
Journal of Nuclear Materials

Journal of Nuclear Materials 499 (2018) 268–271

Contents lists available at ScienceDirect

Journal of Nuclear Materials

journal homepage: www.elsevier.com/locate/jnucmat

The Raman fingerprint of plutonium dioxide: Some example applications for the detection of PuO_2 in host matrices

D. Manara [a, *], M. Naji [a, 1], S. Mastromarino [a, 2], J.M. Elorrieta [a, b], N. Magnani [a], L. Martel [a], J.-Y. Colle [a]

[a] European Commission, Joint Research Centre (JRC), Directorate of Nuclear Safety and Security, P.O. Box 2340, D-76125 Karlsruhe, Germany
[b] Centro de Investigaciones Energéticas, Medioambientales y Tecnológicas, CIEMAT, Avenida Complutense 40, 28040 Madrid, Spain

HIGHLIGHTS

- The Raman fingerprint of PuO_2 is presented and discussed.
- It can be used for the detection of PuO_2 in various environments.
- Several applications are identified.

ARTICLE INFO

Article history:
Received 6 October 2017
Received in revised form
24 November 2017
Accepted 25 November 2017
Available online 26 November 2017

Keywords:
Nuclear materials
Plutonium dioxide
Raman spectroscopy

ABSTRACT

Some example applications are presented, in which the peculiar Raman fingerprint of PuO_2 can be used for the detection of crystalline Pu^{4+} with cubic symmetry in an oxide environment in various host materials, like mixed oxide fuels, inert matrices and corium sub-systems. The PuO_2 Raman fingerprint was previously observed to consist of one main T_{2g} vibrational mode at 478 cm^{-1} and two crystal electric field transition lines at 2130 cm^{-1} and 2610 cm^{-1}. This particular use of Raman spectroscopy is promising for applications in nuclear waste management, safety and safeguard.

The Raman spectrum of crystalline plutonium dioxide has been independently studied by some distinct research groups in the last few years, yielding clear and reproducible results. It has been observed to consist of one main vibrational mode (T_{2g}, at 478 cm^{-1} ± 2 cm^{-1}) and two clear crystal electric field (CEF) transitions at higher energy (2130 cm^{-1} ± 5 $cm^{-1}$and 2610 cm^{-1} ± 5 cm^{-1}), as shown in Fig. 1. The first band, predicted by the Group Theory [1], was observed over forty years ago for the first time in cerium and thorium dioxides [2], and more than twenty years ago in other actinide dioxides, including plutonium dioxide [3]. Although its exact spectral position slightly depends on the chemical nature of the compounds, it can poorly be used to identify single chemical species in complex mixtures. On the other hand, two higher-energy peaks more peculiar of Pu^{4+} with cubic symmetry in an oxide matrix have only been identified and studied in the last few years [4–6]. They have recently been established to be related to $\Gamma_1 \rightarrow \Gamma_5$ and $\Gamma_1 \rightarrow \Gamma_3$ crystal electric field (CEF) transitions, respectively [5,6]. Since in PuO_2 these transitions occur within the ground $^5I_4$ manifold, unlike the $^3H_4$->$^3F_2$ intermultiplet transitions observed for example in UO_2 (cf. [7]), they take place at a relatively low energy and are therefore easily observable in the standard Raman spectra of plutonium dioxide. Their presence makes the Raman fingerprint of PuO_2 quite particular not only among other similar fluorite-like compounds, but also among many other chemical species that can be found in nuclear materials.

If the Raman modes typical of crystalline plutonium dioxide have already been assessed in previous research, the main and original goal of the present work consists in showing some example applications in which the PuO_2 Raman fingerprint has advantageously been used for the detection of crystalline PuO_2 in various

* Corresponding author.
E-mail address: dario.manara@ec.europa.eu (D. Manara).
[1] Current address: Université Sidi Mohamed ben Abdellah, Faculté des Sciences, Département de Physique, B.P. 1796 Atlas Fez, Morocco.
[2] Current address: Nuclear Energy and Radiation Applications (NERA), Radiation, Science & Technology Department, Faculty of Applied Sciences, Delft University of Technology, Mekelweg 15, 2629 JB Delft, The Netherlands.

https://doi.org/10.1016/j.jnucmat.2017.11.042

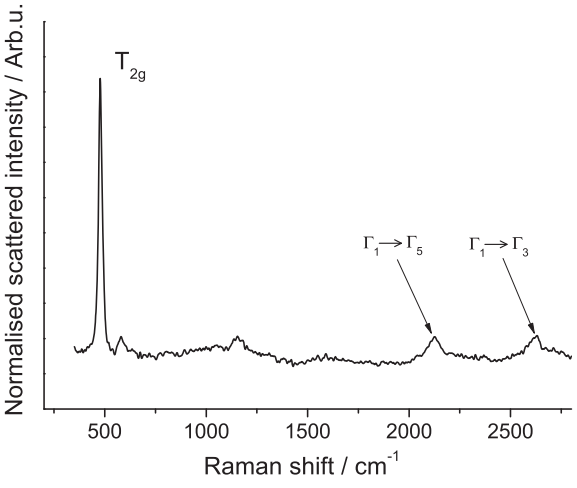

Fig. 1. The Raman spectrum of plutonium dioxide recorded with a 514-nm excitation source. The arrows indicate the electronic modes typical of PuO_2, attributed to $\Gamma_1 \rightarrow \Gamma_5$ and $\Gamma_1 \rightarrow \Gamma_3$ crystal electric field (CEF) transitions.

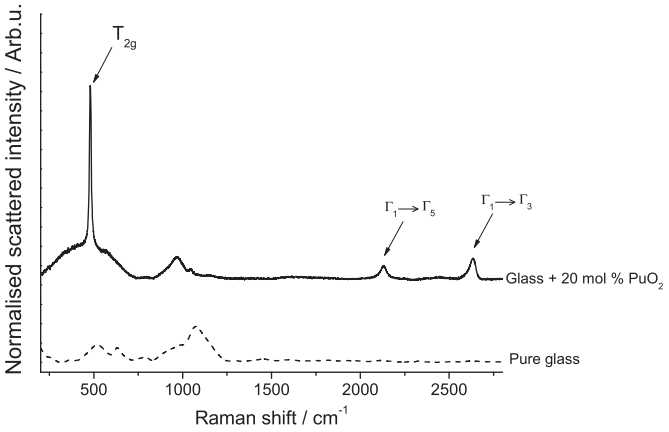

Fig. 2. Raman spectra recorded with a 514-nm excitation source on a sodium-borosilicate glass: pure glass matrix (dotted line) and PuO_2-containing glass (solid line).

environments, inert matrices, corium sub-systems or nuclear waste vitrification glasses. This application of Raman spectroscopy can thus have a large interest in terms of nuclear waste management, safety and safeguard.

Raman spectra have been measured in the present research with the help of a recently developed technique for the confinement of radioactive materials, described elsewhere [8,9] . Such a technique permitted the measurement of heavy alpha emitters in a standard Raman microscope, offering all the flexibility of a non-nuclearized instrument.

The Raman microscope used in this work is equipped with a long working distance (10.6 mm) which offers a 0.5 numerical aperture with a 50 times magnification allowing the acquisition of spectra both on microscopic (up to approximately 2 μm by 2 μm) and macroscopic spots on the sample surface. The Raman spectrometer is a Jobin-Yvon T 64000 equipped with a 1800 grooves per mm grating and a low noise LN2 cooled Symphony® CCD detector. Although the microscope can be coupled to the spectrometer in a confocal mode, this option was not used for the present work. Excitation sources are an Ar^+ Coherent® Continuous Wave (CW) laser with main wavelengths at 488 nm or 514.5 nm or a Kr^+ Coherent® CW laser with main wavelengths at 647 nm or 752 nm, both with a controllable nominal power (up to few W depending on the wavelength) and a monochromator as plasma filter. The excitation source wavelength was chosen case by case depending on the investigated material, in order to maximise the signal-to-noise ratio and minimise fluorescence and sample alteration effects. The power impinging the sample surface is lower by a factor 5 approximately. Using the long focal 50× objective and the single spectrometer mode permits a good spectral resolution (±1 cm^{-1}) independently of the surface shape. The spectrograph is calibrated with the T_{2g} excitation of a silicon single crystal, set at 520.5 cm^{-1} [10]. The instrument is calibrated on a daily basis prior to measurements.

As a first example, Fig. 2 reports the Raman spectrum recorded in this work on a 20 mol % PuO_2-containing sodium borosilicate glass, produced at JRC Karlsruhe in order to simulate the behaviour of nuclear waste vitrification matrices, along with the spectrum of a PuO_2-free glass sample. In addition to some spectral modifications the interpretation of which can be left for further research, the Raman fingerprint of crystalline PuO_2 unambiguously appears, as indicated by the arrows, on the background of the borosilicate glass spectrum for the current PuO_2 concentration. This observation is in line with the precipitation, in the vitreous matrix, of PuO_2 crystallites, indicating that the solubility limit of plutonium dioxide in the glass has been overcome. The analysis can be further refined by extending it to glass samples with various plutonium dioxide contents or to different kind of glasses. This would lead to a more accurate Raman spectroscopy assessment of the PuO_2 solubility in the glass. Moreover, the recently studied Raman spectra characteristic of PuO_2 nano-crystals [11] can be applied to this investigation in order to possibly detect the early appearance of crystalline plutonium-dioxide nano-precipitates, by analysing the T_{2g} peak width and spectral position. Such analysis refinement will be the subject of further research. Independently, the results of the current Raman investigation of PuO_2 – containing borosilicate glasses can be soundly used to detect the presence of crystalline PuO_2 in glasses used for nuclear waste immobilisation.

Another interesting example concerns the detection, by Raman spectroscopy, of Pu^{4+} with cubic symmetry in other oxide matrices of nuclear interest. For example, the black curve in Fig. 3 shows the Raman spectrum of a crystalline zirconium dioxide sample, mixed

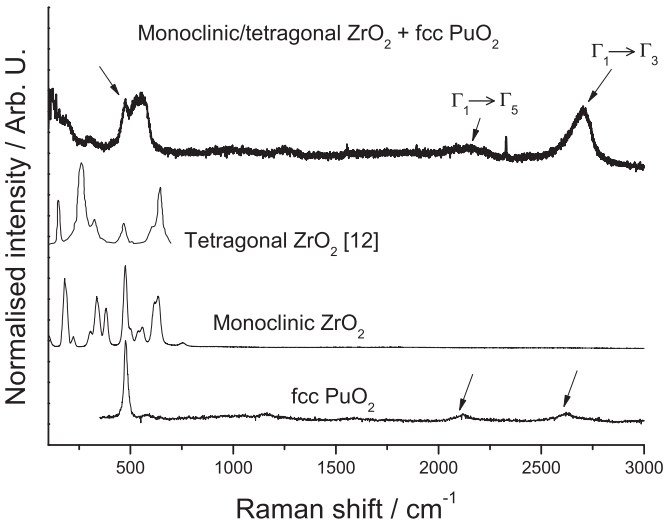

Fig. 3. Raman spectra recorded with a 647-nm excitation source on pure PuO_2, on pure monoclinic ZrO_2, and on a PuO_2-containing monoclinic/tetragonal zirconia matrix. The spectrum of purely tetragonal ZrO_2 has been taken from the literature [12]. Sharp low-intensity peaks in the mixed oxide spectrum are due to oxygen and nitrogen impurities adsorbed on the sample surface.

with a macroscopic (>20 mol %) amount of plutonium dioxide. This sample was obtained by laser-melting a pellet of a pre-sintered mixture of ZrO_2 and PuO_2, in the aim of simulating on a laboratory scale the formation of corium, the melted mixture of nuclear fuel and cladding occurring during a nuclear power plant core meltdown accident. In Fig. 3, the Raman spectrum of PuO_2 is reported together with the spectra of the monoclinic and tetragonal zirconia (the latter one was measured only up to 700 cm^{-1} [12]). Both ZrO_2 allotropies were observed by XRD in the present PuO_2-containing matrix, as it often happens in heat-treated zirconia. It is possible to see, from the Raman spectra of single compounds, that many Raman-active modes overlap in the spectral region between 250 cm^{-1} and 750 cm^{-1}. In particular, the T_{2g} line of PuO_2 at 478 cm^{-1} overlaps almost exactly with a similar line of monoclinic ZrO_2, which makes very difficult the detection of the PuO_2 contribution to the combined spectrum in this range. In this case, the presence of cubic Pu^{4+} in the zirconia matrix can be easily concluded only with the help of the two clear high-energy CEF transition peaks. The different intensities and the slightly varied spectral positions that the two latter peaks display in the zirconia matrix may be due to polarisation effects and to local constraints between PuO_2 and ZrO_2 crystals. Such constraints can be quite complex in this peculiar case, especially when one considers the coexistence of various allotropic forms of zirconia in the investigated material, and the possibility for a partially epitaxial growth, during solidification of the melt, of different crystallites on top of each other. Deepening these aspects goes beyond the scopes of the present communication, and will be left for further more specific research. Nonetheless, Fig. 3 highlights the importance of the two CEF peaks for the sure and prompt detection of the presence of cubic Pu^{4+} in a foreign matrix by Raman spectroscopy, even when the main spectral features of the host matrix largely overlap with the plutonia spectrum at lower energies.

Other examples in which the presence of Pu^{4+} with cubic symmetry can be detected in oxide host matrices are reported in the literature. The work published by Böhler et al. on the ThO_2-PuO_2 system [13] showed that the Raman spectral signature of plutonium dissolved in the fluorite-like crystalline thoria matrix can be detected up to PuO_2 contents in ThO_2 as low as 3 mol %. Like in the previous ZrO_2-PuO_2 case, also here the high energy electronic lines are somewhat shifted and distorted at high dilution, most probably due the large lattice parameter change induced by thoria in the solid solution, with respect with pure plutonia. Böhler et al. noticed that the ratio between the spectral position of the CEF lines and that of the "mixed" T_{2g} line remained almost constant for all the (Th, Pu)O_2 investigated compositions. This behaviour is normal when it is considered that plutonia is largely soluble in thoria [14], and a distortion of the crystal electric field can be logically expected in the solid solution. Raman spectra have been recorded in this work on similar samples, plutonia-containing thorium dioxide with increasing PuO_2 content, starting from 3 mol % of PuO_2. They are reported in Fig. 4. It can be noticed that the very intense T_{2g} line is shifted at different compositions. In all the cases, the presence of Pu^{4+} with cubic symmetry in the thoria matrix is obviously detected by the presence of the high-energy CEF transition peaks, indicated by arrows in Fig. 4. The attribution of other Raman lines present in the spectra of Fig. 4 is reported in Ref. [13].

Another interesting example can be found in the investigation performed by Sarsfield et al. [4], in which the Raman fingerprint of PuO_2 reveals the progressive formation of crystalline plutonia, or at least of Pu^{4+} with cubic symmetry, upon laser heating-induced decomposition of plutonium (VI) hydroxide. This kind of information, once more accessible with the sole help of Raman spectroscopy and the PuO_2 Raman fingerprint, is useful for the analysis of nuclear waste chemical stability.

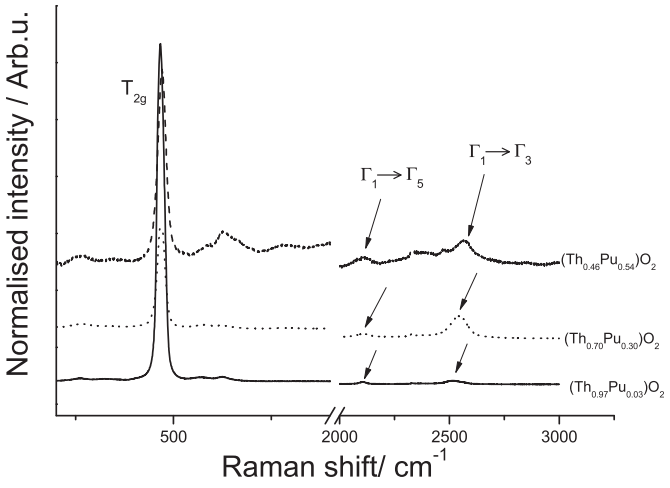

Fig. 4. Raman spectra recorded with a 647-nm excitation source mixed $ThO_2 - PuO_2$ oxides. The spectra are truncated between 900 cm^{-1} and 2000 cm^{-1} for a better readability.

It is important to notice here, that distortion and shift of the current CEF Raman peaks are generally observed in samples where cubic Pu^{4+} is dissolved in an oxide solid solution or epitaxial crystalline PuO_2 grows on another crystalline matrix, as opposed to the case where pure PuO_2 crystallites precipitate from the material matrix, for example the vitreous one of Fig. 1. The CEF peak shift amounts to a dozen of cm^{-1} at most for the $\Gamma_1 \rightarrow \Gamma_5$ line and to a couple of dozens of cm^{-1} for the $\Gamma_1 \rightarrow \Gamma_3$ one. Raman peaks are observed to broaden by a few cm^{-1} in both modes. In all cases, unambiguous detection of the Raman fingerprint of Pu^{4+} with cubic symmetry in an oxide environment is ensured by the simultaneous observation of the T_{2g} mode close to 478 cm^{-1} and the two CEF lines around 2130 cm^{-1} and 2610 cm^{-1}.

In summary, it is evident, from the recent research results reported here, that the newly assessed Raman fingerprint of crystalline PuO_2 can be conveniently employed for the detection of plutonia and, more in general, of cubic Pu^{4+} in different types of oxide environments. In the light of the flexibility offered by Raman spectroscopy, which can be used both as an in-situ and ex-situ analysis technique (cf. [15]), this fingerprint is potentially an extremely useful tool for many applications. It can indeed be employed for the detection of cubic Pu^{4+} oxide hotspots in various situations of interest for the nuclear safeguard, the analysis of nuclear waste, the investigation of corium produced in nuclear plant meltdown accidents, the detection of illicit traffic of nuclear materials, etc.

Acknowledgements

The Authors are indebted to J. Boshoven (JRC Karlsruhe) for the preparation of samples analysed in this work and to M. Sierig (JRC Karlsruhe) for his assistance in the Raman spectrum measurements. They moreover wish to acknowledge R. Caciuffo, R. Konings and J. Somers (JRC) for their highly valuable scientific advice. S.M. and J.M.E. acknowledge the EURATOM FP7 project GENTLE (contract number 323304) for supporting their stay at JRC Karlsruhe.

References

[1] T. Shimanouchi, M. Tsuboi, T. Miyazawa, Optically active lattice vibrations as treated by the GF-Matrix method, J. Chem. Phys. 35 (1961) 1597, https://doi.org/10.1063/1.1672186.
[2] V.G. Keramidas, W.B. White, Raman spectra of oxides with the fluorite structure, J. Chem. Phys. 59 (1973) 1561, https://doi.org/10.1063/1.1680227.

[3] G.M. Begun, R.G. Haire, W.R. Wilmarth, J.R. Peterson, Raman spectra of some actinide dioxides and of EuF_2, J. Less Common Met. 162 (1990) 129, https://doi.org/10.1016/0022-5088(90)90465-V.
[4] M.J. Sarsfield, R.J. Taylor, C. Puxley, H.M. Steele, Raman spectroscopy of plutonium dioxide and related materials, J. Nucl. Mater 427 (2012) 333, https://doi.org/10.1016/j.jnucmat.2012.04.034.
[5] F. Gendron, J. Autschbach, Puzzling lack of temperature dependence of the PuO2 magnetic susceptibility explained according to ab intio wave function calculations, J. Phys. Chem. Lett. 8 (3) (2017) 673, https://doi.org/10.1021/acs.jpclett.6b02968.
[6] M. Naji, N. Magnani, L.J. Bonales, S. Mastromarino, J.-Y. Colle, J. Cobos, D. Manara, Raman spectrum of plutonium dioxide: vibrational and crystal field modes, Phys. Rev. B 95 (2017) 1043071–1043077, https://doi.org/10.1103/PhysRevB.95.104307.
[7] T. Livneh, Coupling of multi-LO phonons to crystal-field excitations in UO_2 studied by Raman spectroscopy, J. Phys. Condens. Matter 20 (2008) 085202, https://doi.org/10.1088/0953-8984/20/8/085202.
[8] M. Naji, J.-Y. Colle, O. Benes, M. Sierig, J. Rautio, P. Lajarge, D. Manara, An original approach for Raman spectroscopy analysis of radioactive materials and its application to americium-containing samples, J. Raman Spectrosc. 46 (2015) 750, https://doi.org/10.1002/jrs.4716.
[9] J.-Y. Colle, M. Naji, M. Sierig, D. Manara, A novel technique for Raman analysis of highly radioactive samples using any standard micro-Raman spectrometer, J. Vis. Exp. (2017) 122, https://doi.org/10.3791/54889 e54889.
[10] H. Richter, Z. Wang, L. Ley, The one phonon Raman spectrum in microcrystalline silicon, Solid State Commun. 39 (1981) 625, https://doi.org/10.1016/0038-1098(81)90337-9.
[11] D. Hudry, C. Apostolidis, O. Walter, A. Janßen, D. Manara, J.-C. Griveau, E. Colineau, T. Vitova, T. Prüßmann, D. Wang, C. Kübel, D. Meyer, Ultra-small plutonium oxide nanocrystals: an innovative material in plutonium science, Chem. Eur. J. 20 (2014) 10431–10438, https://doi.org/10.1002/chem.201402008.
[12] J.A. Muñoz Tabares, M.J. Anglada, Quantitative analysis of monoclinic phase in 3Y-TZP by Raman spectroscopy, J. Am. Ceram. Soc. 93 (2010) 1790–1795, https://doi.org/10.1111/j.1551-2916.2010.03635.x.
[13] R. Böhler, P. Çakır, O. Bene, H. Hein, R.J.M. Konings, D. Manara, High temperature phase transition of mixed (PuO_2 + ThO_2) investigated by laser melting, J. Chem. Thermodyn. 81 (2015) 245–252, https://doi.org/10.1016/j.jct.2014.10.006.
[14] S. Hubert, J. Purans, G. Heisbourg, P. Moisy, N. Dacheux, Local structure of actinide dioxide solid solutions $Th_{1-x}U_xO_2$ and $Th_{1-x}PuxO_2$, Inorg. Chem. 45 (2006) 3887–3894. https://doi.org/10.1021/ic050888y.
[15] D. Ho Mer Lin, D. Manara, T. Fanghänel, K. Mayer, The use of different dispersive Raman spectrometers for the analysis of uranium compounds, Vibr. Spectrosc. 73 (2014) 102–110. https://doi.org/10.1016/j.vibspec.2014.05.002.